



Institute of Paper Science and Technology
Atlanta, Georgia

IPST TECHNICAL PAPER SERIES



NUMBER 421

**A TECHNIQUE FOR QUANTITATIVE MEASUREMENTS
OF SHEAR RATE AND FLOW CHARACTERISTICS
IN COATING SYSTEMS**

J.D. BENSON AND C.K. AIDUN

FEBRUARY 1992

**A Technique for Quantitative Measurements
of Shear Rate and Flow Characteristics in Coating Systems**

J.D. Benson and C.K. Aidun

**To be submitted to
TAPPI Coating Conference
Orlando, Florida
May 1992**

Copyright© 1992 by The Institute of Paper Science and Technology

For Members Only

NOTICE & DISCLAIMER

The Institute of Paper Science and Technology (IPST) has provided a high standard of professional service and has put forth its best efforts within the time and funds available for this project. The information and conclusions are advisory and are intended only for internal use by any company who may receive this report. Each company must decide for itself the best approach to solving any problems it may have and how, or whether, this reported information should be considered in its approach.

IPST does not recommend particular products, procedures, materials, or service. These are included only in the interest of completeness within a laboratory context and budgetary constraint. Actual products, procedures, materials, and services used may differ and are peculiar to the operations of each company.

In no event shall IPST or its employees and agents have any obligation or liability for damages including, but not limited to, consequential damages arising out of or in connection with any company's use of or inability to use the reported information. IPST provides no warranty or guaranty of results.

A Technique for Quantitative Measurements of Shear Rate and Flow Characteristics in Coating Systems

John D. Benson and **Cyrus K. Aidun**
Assistant Engineer Assistant Professor

Institute of Paper Science and Technology
575 14th Street, N.W.
Atlanta, Georgia 30318

ABSTRACT

The flush-mounted hot-film anemometer (FMHFA) may be used to investigate the flow characteristics in coating systems. This device has a hot-film sensor heated by an electric current and cooled by the incidental flow, which acts by virtue of its mass flux and its temperature. With this system, we measure the current (or resistance) which correlates with the wall shear rate. The resulting heat transfer between the hot-film sensor and the fluid is detected electrically as a function of flow parameters. We have used this setup to obtain quantitative measurements of the critical machine speed, or the critical Reynolds number, for the transition from steady-state to time-periodic and unsteady flow in a cavity simulating the pond of a short-dwell coater. The results confirm the previous flow visualization experiments and provide additional information on the dynamics of the system and the shear rate in the cavity. The technique developed in this study can be used to measure the wall shear rate in any coating system. This technique is nonintrusive, relatively easy to apply, and can be used with opaque fluids such as coating colors.

KEYWORDS: Flush-Mounted Hot-Film Anemometer, Constant Temperature Anemometer, Coating, Blade Coaters, Shear Rate, Fluid Dynamics, Rheology.

I. INTRODUCTION

Hot-film and hot-wire anemometers are devices used to measure any possible parameter occurring in steady and unsteady flows, such as shear rate, velocity, turbulence (separation-reattachment process). This technique has been applied to flows in wind tunnels (1, 2), pulsatile pipe flows (3), and artificial aortic valves (4, 5, 6, 7). This technique is ideal for application to coating systems. Nandy and Tarbell (8) are the only investigators to use HFA for both Newtonian and non-Newtonian fluids. They used a flush-mounted hot-film anemometer (FMHFA) to measure the wall shear stress in the vicinity of an Ionescu-Shiley trileaflet valve, which simulates the functioning of a human aortic valve. In their results, they found that for Newtonian fluid, the peak wall shear rate decreases significantly with increasing distance from the entrance of the aortic valve channel (or valve seat). They attribute this to the flow becoming fully developed as it gets further away from the valve seat. For non-Newtonian fluid, they discovered the opposite trend. Here, the peak wall shear rate increases with distance from the valve seat. However, they do not give a definite conclusion for this difference in wall shear values for Newtonian and non-Newtonian fluids since limited data were available to them in their preliminary study. Reed et al. (9) have used the HFA to determine the local velocity in liquid-metal (mercury at room temp.) magnetohydrodynamic experiments for fusion blanket applications. They concluded that HFA was chemically compatible with liquid metals and proved to be a powerful and quantitative tool for local velocity measurements. With the exception of Nandy et al. and Reed et al., HFA studies for non-Newtonian fluids and fluids with suspensions are very limited.

The hot-film sensor we have used is made of a thin metallic film. It is heated by an electric current and cooled by the incidental flow, which acts by virtue of its mass flux and its temperature (10). Using the hot-film sensor, which is sensitive to flow conditions, one can measure the current (or resistance) and then be able to deduce any possible information about the flow. The resulting heat transfer between the hot-film sensor and the fluid is detected electrically as a function of flow parameters (11). In our experimental setup, the hot-film sensor is included in a Wheatstone bridge circuit. The offset voltage is amplified and fed back to the bridge to restrain the resistance changes of the hot-film sensor. A balanced bridge implies that the sensor resistance, R_s , is constant, and therefore, the sensor

temperature is constant. It is for this reason that this system is called a constant temperature anemometer (CTA) (12). The probe is connected to the terminals of A and B as shown in Figure 1. Depending upon the operating fluid temperature, a control value resistor is placed across CD. The output terminal EF can be connected to a chart recorder or data acquisition system. Terminal GH is connected to a power supply (+15 V, 0.7 amps) and ground. After all connections are made, the bridge voltage should vary with the flow past the sensor.

Figure 2 shows a typical cylindrical FMHFA sensor and probe. The sensor, which is about 0.1 mm^2 in area, is flush with one end of the cylinder. Two platinum wires are connected to the ends of the flushed sensor and are enclosed inside of the cylindrical probe. These two wires extend out to the other end of the cylinder (right side of Figure 2) and connect to a probe holder, which inputs a voltage signal across AB of the Wheatstone bridge circuit.

The FMHFA can be used to study the behavior of flow in some coaters in the paper industry, such as the short-dwell coater and flexible blade coater, for various fluids and coating colors. It can also be used to determine the stability properties of flow in the pond of a coater. In our studies, new results with a flush-mounted hot-film anemometer have confirmed earlier results found in flow visualization studies of a cavity simulating the pond of a short-dwell coater (SDC) (13, 14).

II. CALIBRATION TECHNIQUES

The calibration of the FMHFA is usually made under steady flow conditions, and it is assumed that these calibrations will apply to quasisteady (15) and to unsteady (16) flow conditions. It has been found in the current literature that most FMHFAs have been calibrated using steady Couette flow (16, 17). Tillmann and Schlieper have calibrated a FMHFA using two concentric cylinders with the outer one rotating at a known, constant velocity. This establishes a laminar Couette flow within the gap. The stationary inner cylinder holds the probe and measures representative results for shear stresses in the range from 1.3 to 30 N/m^2 . The known shear stress of the fluid is then correlated and plotted versus the hot-film sensor readings.

Another method for calibrating the FMHFA is using Poiseuille's flow in a pipe, which has been attempted by Nandy and Tarbell (18). This is the method that is used in our study. In this case, the hot-film sensor is mounted flush with the inside tube wall of a long pipe. The flow in the test section is steady and fully developed. The shear stress is proportional to the pressure difference across the pipe, so the hot-film sensor reading is plotted versus the shear stress at the wall.

The FMHFAs are designed to be mounted flush with a surface or wall, where the flow is perpendicular to the axis of the probe body. It has been found that there will be as much as a 20% deviation in the hot-film anemometer bridge voltage with a change in probe position of 9% of the probe diameter from the wall. This could result in a 50% error in computed wall shear stress (19). Therefore, it is of extreme importance to position the hot-film sensor as flush with a wall or surface as possible. One possible way to position the probe accurately is to install a micrometer on top of the probe, thus moving the probe an exact distance equal to the thickness of the pipe wall (19).

The necessary equipment used in calibrating the hot-film anemometer consists of an 11-foot, 3/4-inch diameter plexiglass pipe mounted on a flat surface. There are two reasons for using a transparent pipe. The first is to ensure that we have visually obtained steady-state flow. The second reason is to assure that the probe surface is flush with the inside wall of the tube. Before the measurements of the pressure difference across the pipe are made, an entry length of four feet was allowed, using the entry flow length given by Langhaar (20) $L = 0.057(Re)d$, where Re is the Reynolds number, and d is the pipe diameter. The length between the two pressure ports (P1 and P2) is five feet. A pressure differential transducer used in this experiment provides a DC output voltage linearly proportional to the applied pressure. Recording the pressure difference across the pipe is necessary since the pressure difference is linearly proportional to shear stress given by:

$$\tau = r_0 \Delta p / 2L$$

where r_0 is the radius of the pipe, and L is the distance between the pressure ports (see Figure 3).

The FMHFA is placed halfway between the two pressure ports. The hot-film sensor, which is perfectly flush with the inside tube wall, is .127 by 1.016 mm in size. The output signal from the hot-film sensor is received by a constant temperature anemometer. The main purpose of this constant temperature anemometer is to transmit high-level signals from the hot-film sensor into a voltage signal, which can be measured on any chart recorder or data acquisition system.

In our calibration setup, the heat transfer between the hot-film sensor and the fluid is detected electrically as a function of shear stress. The constant temperature anemometer system operates on a +15 VDC (.7 amps) power supply. The probe, which holds the hot-film sensor and is 3.2 mm in O.D., is designed to be mounted flush with a surface or wall, where the flow is perpendicular to the axis of the probe body. The data collected from the hot-film sensor are recorded in volts with a data acquisition system connected to an IBM-PC. During the calibration experiment, the pressure difference across the pipe and the shear stress reading from the hot-film anemometer are recorded during each change in temperature of the fluid. The temperature of the fluid steadily increases from 20° C to 25 ° C, and Δp readings are taken with every 0.2 ° C increase in temperature. Since the hot-film sensor is very sensitive to temperature changes, a thermistor was installed next to the probe. Thus, the data acquisition system collects three parameters for the calibration setup: the hot-film sensor signal, temperature, and pressure difference.

After all readings are taken, the actual shear stress is calculated from the given equation for τ and plotted versus the hot-film sensor reading in millivolts. Calibration graphs have to be plotted for every change in temperature since the hot-film sensor output varies linearly with temperature. Since temperature change is proportional to both shear stress and viscosity of the fluid, it was found experimentally that as temperature increases, shear stress decreases. The main purpose of these calibration graphs is their use as a reference chart when the hot-film anemometer is used in actual experimental measurements of the shear stress at the wall of a cavity simulating the pond of a short-dwell coater. For example, if the reading of the hot-film sensor is 2100 mV at 20° C, the actual shear stress will be 34 N/m² at that point (see Figure 4). The calibration curves can be used for unsteady flows as long as the time scale of the flow is much larger than the HFA response time. This is the case for most coating flow problems.

III. FMHFA WITH NON-NEWTONIAN FLUIDS

As mentioned earlier, HFA studies for non-Newtonian fluids are very limited and to date have been reported only by Nandy and Tarbell (8). With their preliminary studies, they have proved that the HFA can be a useful tool for both, Newtonian and non-Newtonian fluids. In calibrating the hot-film probe, the simple theory of fully-developed flow of a power law fluid in a rigid straight tube can be applied here. For this fluid, the wall shear rate (S) is proportional to the flow rate (Q) and inversely proportional to the power law exponent (n) and the cube of the tube radius (R) as shown below (8):

$$S = Q/\pi R^3 [3 + 1/n]$$

Knowing (n) from viscosity calibration of a fluid sample (best fit power law equation for shear stress vs. shear rate) and R as a constant, the wall shear rate (S) can then be calculated from collecting measurements of the flow rate (Q). Thus, the HFA can be a useful tool when using various coating colors and opaque coating fluids, all of which are non-Newtonian.

IV. APPLICATIONS TO A CAVITY SIMULATING THE POND OF A SHORT-DWELL COATER

Understanding the stability properties of flow in a cavity simulating the pond of a SDC is important because of fundamental and practical reasons. A number of complex coating systems are found in the pulp and paper industry, such as short-dwell coaters (SDC) (21, 22, 23) and flexible blade coaters (22, 24) used for production of high-grade paper and photographic films. Short-dwell blade coaters have efficiently increased productivity and give desired coating properties such as uniform thickness. However, the trend to increase machine (roll) speed while minimizing coat weight is hindered by the difficulty of maintaining a uniform coat weight profile across the reel (25, 26, 27). Monitoring the stability properties of flow in coating systems is critical so that nonuniform coating may be prevented.

Short-dwell coaters have gained acceptability in the coating industry due to their compactness, operational capability, and increased productivity. However, many aspects of the flows which occur in SDC are not well understood. For example, at high-roll speeds, rapid variations within the flow can occur, thereby causing wet-film thickness nonuniformities which are outside of the statistically acceptable limits. Furthermore, these rapid changes can cause "ribbings," (26) or streaks, on the finished product. Ribbings, or streaks, in coating systems are usually defined as an uneven or nonuniform coat weight profile in the cross direction of the reel. These nonuniform coating thicknesses have 20% to 60% less coat weight than the uniform coating thickness area across the reel (see Figure 5). These deficiencies usually vary from two to eight centimeters wide. This is a condition which cannot be tolerated in the manufacturing of commercial paper products. A hot-film anemometer is an effective tool for determining the pond's hydrodynamic state.

We have used the hot-film anemometer technique for measurements of the cavity flow simulating the pond of a SDC. Mounted flush with the inside wall of the cavity, the probe and thermistor are both installed adjacent to each other. The quantitative data analysis also includes the flow rate feeding into the cavity. Using a data acquisition system, all of these parameters (temperature, flow rate, hot-film sensor) are collected at a sampling rate of 10 Hz, and only the hot-film sensor is collected at 100 Hz.

Starting at the Reynolds number of about 200, the data are collected by the data acquisition system in increasing Re intervals of about 30 until Re reaches about 1300. Viscosity and fluid temperature readings are both taken at every interval in the Reynolds number range of 200 to 1300. After each experimental run, the data can be analyzed on a software program. A commercial software was used to obtain the Fast Fourier Transformation (FFT) of the signal. By performing a FFT on the available data, we can determine the dynamical state of the flow in the pond.

V. RESULTS

The first set of our experiments is with the probe located 12 mm from the bottom wall of the cavity. This positions the probe right below the top of the downstream secondary eddy (DSE) (25). Four experiments are completed at this probe position. The

second set of experiments is run with the probe moved to a lower position, 4 mm from the bottom wall. Three experiments are completed at this second position. Figure 6 shows the hardware of the probe and its holder located at the second position of the plexiglass cavity.

Since our experiments give the same results for both probe positions, only the experiment with the probe located 12 mm from the bottom wall will be discussed. In this and all other experiments, the hot-film anemometer was collected from the data acquisition system at sampling rates of 10 and 100 Hz. However, the temperature and the flow rate into the cavity were collected only at a 10 Hz sampling rate. Since the flow rate and temperature frequency remain constant with increasing the Reynolds number, it was reasonable to plot the dimensionless frequency of the flow rate at 10 Hz and the hot-film sensor at 100 Hz as shown in Figure 7. A plot of all the parameters at a 10 Hz sampling rate will show the same results as that in Figure 7. It is interesting to note that the hot-film anemometer will detect even small disturbances in the flow field. Figure 7 shows that at $263 < Re < 908$, the Strouhal number of the flow rate, $F.R.f_1/f^*$, and hot-film anemometer, f_1/f^* , overlap perfectly at about 0.027. The Strouhal number is equal to the fundamental frequency found on the FFT graph times the depth of the cavity and divided by the roll speed. An example of this FFT graph is shown in Figure 8.

It may be noted that there is a breaking point where the hot-film anemometer signal does not follow along the flow rate frequency, but instead jumps to detect a second frequency at 0.115 which corresponds to transition from steady to periodic (limit cycle) state. Figure 7 shows that at $Re > 900$, the time periodicity due to flow instability is independent of the transients due to temperature and flow rate. Through additional experiments, we have also determined that the second frequency is due to flow instability and is independent of the interaction of other frequencies present in the system.

Figure 9 shows the power spectrum at several values of the Reynolds number. At $Re < 900$ (Figure 9a), the only peaks that appear are due to disturbances caused by the slow fluctuations in temperature and flow rate. These disturbances are orders of magnitude smaller than the actual flow and, therefore, for all practical purposes, the flow is steady state. At $Re \sim 935$ (Figure 9b), a fundamental frequency appears at $f \sim 2.3193$ Hz. This frequency indicates a dynamical transition due to flow instability in the pond. The small-scale disturbance frequencies at $f \sim 0.1099$ and 0.5371 Hz are due to fluid temperature

variation and flow rate feeding into the pond, respectively. Thus, the FMHFA is sensitive enough to detect even small disturbances in the flow field. A new change occurs at $992 < Re < 1089$ in which the flow becomes quasi-periodic! Since the frequency at $f \sim 0.1221$ Hz at $Re \sim 992$ has such a large scale on the FFT power spectrum, we determined that it must be due to the change in flow behavior at the DSE. The power spectrum increases as the Reynolds number increases beyond $Re \sim 1000$ as shown in Figure 9(e,f). A step-by-step progression of the FFT graphs in the range $935 < Re < 1089$ is shown by Figure 9. The mode of transition in this system from steady to unsteady state and turbulence is of fundamental importance and will be fully discussed in a future publication (29).

VI. CONCLUSION AND DISCUSSION

As shown below in Figure 10, hot-film anemometry has confirmed the past flow visualization results in determining the transition to a time-periodic state in a through-flow lid-driven cavity at about $Re \sim 800$. In general, the quantitative measurements detect the transition at a slightly lower Reynolds number than flow visualization does. The objective of this work was to prove the usefulness of hot-film anemometry in detecting flow instability in coating systems.

The use of hot-film anemometry has proven to be a good tool in studying the flow behavior in a cavity simulating the pond of a SDC. With this technique, we have detected a second transition from time-periodic to a quasi-time-periodic state. The results from the HFA suggest that the crude measurements of the frequency by visual inspection may not be correct. The actual frequency of oscillation at the onset of time-periodic state is much larger than what was reported by visual inspection.

A brief discussion is considered here on the relationship between the transition from steady-state to unsteady flow and cross direction nonuniformities of coating on thin paper and photographic films. When the flow becomes unsteady at the DSE, the primary eddy in turn "feels" this instability. The primary eddy, as observed from flow visualization, forms thin vertical lines which follow the movement of the time-periodic waves at the DSE. These vertical lines in turn may affect the coating process causing streaks and patches. Therefore, these streaks and patches could be caused entirely by the three-dimensional

hydrodynamic instability in the pond of coating applicators. Other possibilities are explained by Miura and Aidun (28).

One simple application of hot-film anemometry would be to apply it on-line to high-speed coaters. It could be used to monitor the flow instability or shear rate in the coating applicators. A process could be developed in which the signal from the hot-film anemometer is continually analyzed on a high-speed computer (see Figure 11).

BIBLIOGRAPHY

1. J. Davidson and M. Ritsch, ASCE Eng. Mech. Specialty Conf. on Mech. Comput. in 1990s and Beyond, Conf. in Columbus, Ohio, "Gas Phase Turbulence Modification with Fine Particles in 2-D Duct Flow." 378-382, 1991.
2. R. Thunker, W. Nitsche, and M. Swoboda, Inter. Cong. on Instrum. in Aerosp. Simu. Facilities, Publ by IEEE, Piscataway, N.J., "Hot-Wire, Hot-Film and Surface Hot-Film Applications in Strongly Temperature Loaded Flows." 434-42, 1989.
3. C.L. Tock, ASME, Bioeng. Div., "Onset of Transition in Pulsatile Pipe Flow." 17, 369-71, 1990.
4. H. Nygaard, M. Giersiepen, J.M. Hasenkam, D. Westphal, P.K. Paulsen, H. Reul, J. Biomech., "Estimation of Turbulent Shear Stesses in Pulsatile Flow Immediately Downstream of Two Artificial Aortic Valves in Vitro." 23 (12), 1231-38, 1990.
5. J.M. Hasenkam, H. Nygaard, M. Giersiepen, H. Reul, H. Stodkilde-Jorgensen, J. Biomech., "Turbulent Stress Measurements Downstream of Six Mechanical Aortic Valves in a Pulsatile Flow Model." 21 (8), 631-45, 1988.
6. J.T Baldwin, J.M. Tarbell, S. Deutsch, D.B. Geselowitz, IEEE, 9th Engin. in Medic. and Biol. Soc. Ann. Conf., Boston, MA, "Wall Shear Stress Measurements Within an Artificial Heart Ventricle." 1189-91, 1987.
7. J.T. Baldwin, D. Francischelli, J.M. Tarbell, S. Deutsch, D.B. Geselowitz, ASME, Applied Mech. Div., Conf. Paper Presented at the 3rd Joint ASCE/ASME Mechanics Conf. in San Diego, CA, "Fluid Mechanics of the Penn State Artificial Heart: LDA and Dye Washout Studies." 257-60, 1989.
8. S. Nandy and J.M. Tarbell, Biorheology, "Flush-Mounted Hot-Film Anemometer Measurement of Wall Shear Stress Distal to a Tri-leaflet Valve for Newtonian and Non-Newtonian Blood Analog Fluids." 24, 483-500, 1987.

9. C.B. Reed, B.F. Picologlou, P.V. Dauzvardis, J.L. Bailey, Fusion Technol., "Techniques for Measurements of Velocity in Liquid-Metal MHD Flows." **10** (3), 813-21, 1986.
10. G. Comte-Bellot, Annual Review of Fluid Mechanics, "Hot Wire Anemometry." **8**, 209-31, 1976.
11. S.C. Ling and P.G. Hubbard, J. of the Aeronautical Sciences, "The Hot-film Anemometer: A New Device for Fluid Mechanics Research." **23**, 890-891, September, 1956.
12. L.M. Fingerson, Paper presented at the Symposium on Turbulence in Liquids. University of Missouri-Rolla, "Parameter for Comparing Anemometer Response." October 4-6, 1971.
13. J.D. Benson, M.S. Thesis, Georgia Institute of Technology, Atlanta, GA, "Transition to a Time-Periodic State in a Through-Flow Lid-Driven Cavity." 1991.
14. J.D. Benson and C.K. Aidun, Bulletin of the American Physical Society, "Transition to a Time-Periodic State in a Through-flow Lid-Driven Cavity." **36** (10), 1991.
15. M.R. Davis, J. of Physics E: Scientific Instruments, "The Dynamic Response of Constant Resistance Anemometers." **3**, 15-20, 1970.
16. W. Tillmann and H. Schlieper, J. of Physics E: Scientific Instruments, "A Device for the Calibration of Hot-Film Wall Shear Probes in Liquids." **12**, 373-380, 1979.
17. W. Tillmann, M. Waschmann, M. Herold, and G. Häubinger, J. of Physics E: Scientific Instruments, "Hot-film Wall Shear Probe for Measurement at Flexible Walls." **14**, 692-694, 1981.
18. S. Nandy and J.M. Tarbell, J. Biomechanical Eng., "Flush-Mounted Hot Film Anemometer Accuracy in Pulsatile Flow." **108**, 228-231, 1986.

19. G.E. Miller, *J. of Physics E: Scientific Instruments*, "Position Sensitivity of Hot-Film Shear Probes." **13**, 973-976, May 1980.
20. H.L. Langhaar, *J. of Applied Mechanics*, "Steady Flow in the Transition Length of a Straight Tube." **9**, 55-58, 1942.
21. C.K. Aidun and N.G. Triantafillopoulos, *Int. Symp. Mech. Thin-Film Coating*, Spring National Meeting of the AIChE, "Global Stability Properties of Flow in the Pond of a Short Dwell Coater." March 18-22, 1990.
22. D.E. Eklund and P.C. Norrdahl, *Coating Conference Proceedings*, TAPPI Press, Washington, D.C., "The Flow Characteristics in a Short Dwell Coater." 99-103, 1986.
23. H. Affes, A.T. Conslisk, and M.R. Foster, *Coating Conference Proceedings*, TAPPI Press, Boston, MA, "The Steady Flow in a Short Dwell Coater." 299-307, 1990.
24. G.L. Booth and N. Millman, *TAPPI Monograph Ser. no. 28*, "Pigment Coating Processes for Paper and Board." New York, 1965.
25. N.G. Triantafillopoulos, Ph.D. Thesis, Institute of Paper Science and Technology, Atlanta, GA "Fluid Dynamics of Short-Dwell Blade Coater Ponds and Their Relationship to Cross Directional Coat Weight Nonuniformities." 1991.
26. N.G. Triantafillopoulos and C.K. Aidun, *Tappi J.*, "Relationship Between Flow Instability in Short Dwell Coater Ponds and Cross Directional Coat Weight Nonuniformities." **73(6)**, 129, 1990.
27. H.P. Sollinger, *Coating Conference Proceedings*, Tappi Press, Boston, MA, "New Developments in Coating CD Profile Control." 347-351, 1990.
28. H. Miura and C.K. Aidun, *TAPPI Coating Conference Proceedings*, "Effects of CD Pressure Variations on Coat-Weight Nonuniformities," May 1992.

29. J. Benson and C.K. Aidun, "Transition to Unsteady State in a Lid-Driven Cavity with Throughflow," under preparation.

ACKNOWLEDGMENT

This project was supported by the member companies of the Institute of Paper Science and Technology. Some of the equipment used was generously donated to IPST by Beloit Corporation. Portions of this work were used by JDB as partial fulfillment of the requirements for the M.S. degree at the School of Mechanical Engineering at Georgia Institute of Technology.

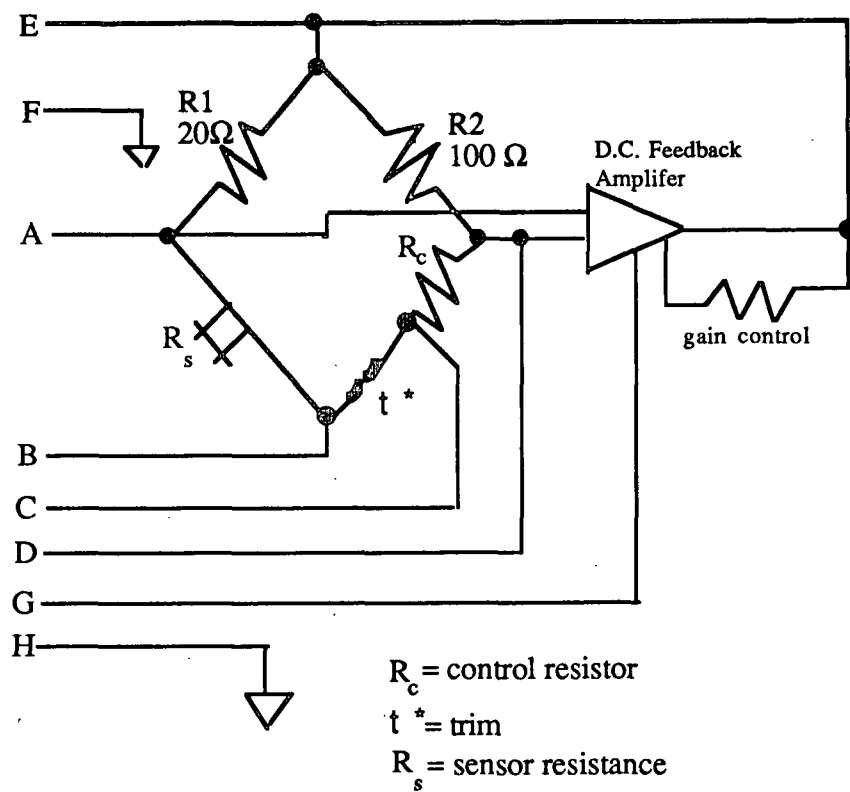


Figure 1. Constant Temperature Anemometer (CTA) Wheatstone Bridge Circuit.

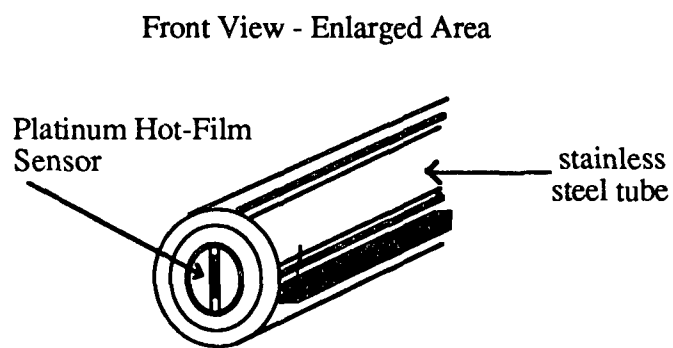
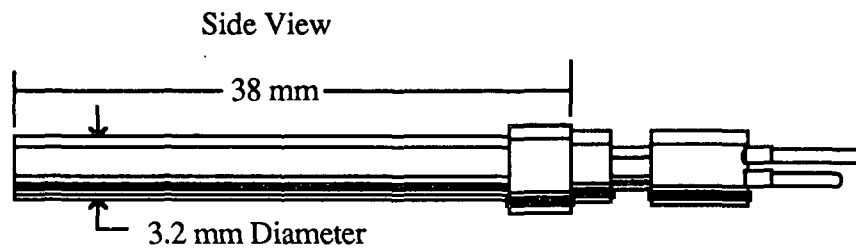


Figure 2. Flush-Mounted Hot-Film Anemometer Schematic.

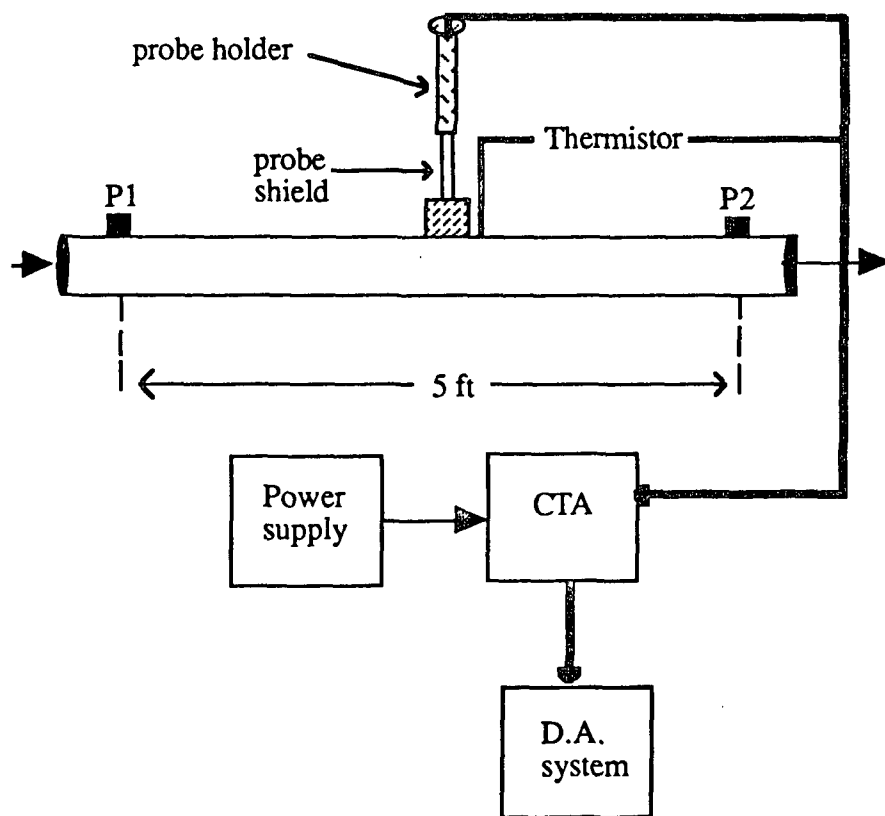


Figure 3. FMHFA Calibration Setup (not at full scale).

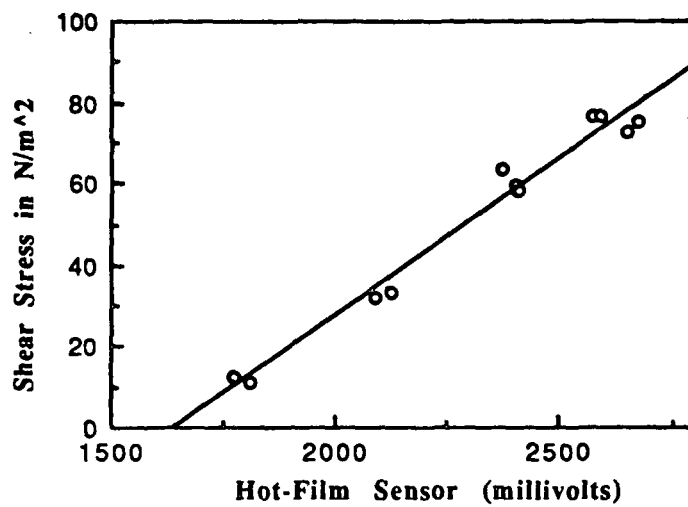


Figure 4. Hot-Film Sensor Calibration Graph @ 20°C.

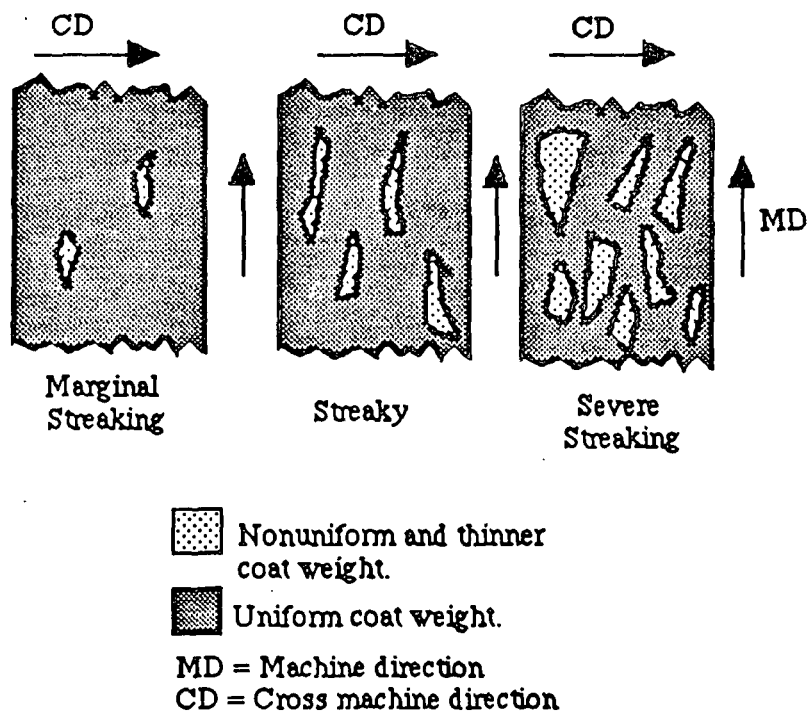


Figure 5. Cross Direction Nonuniformity Design.

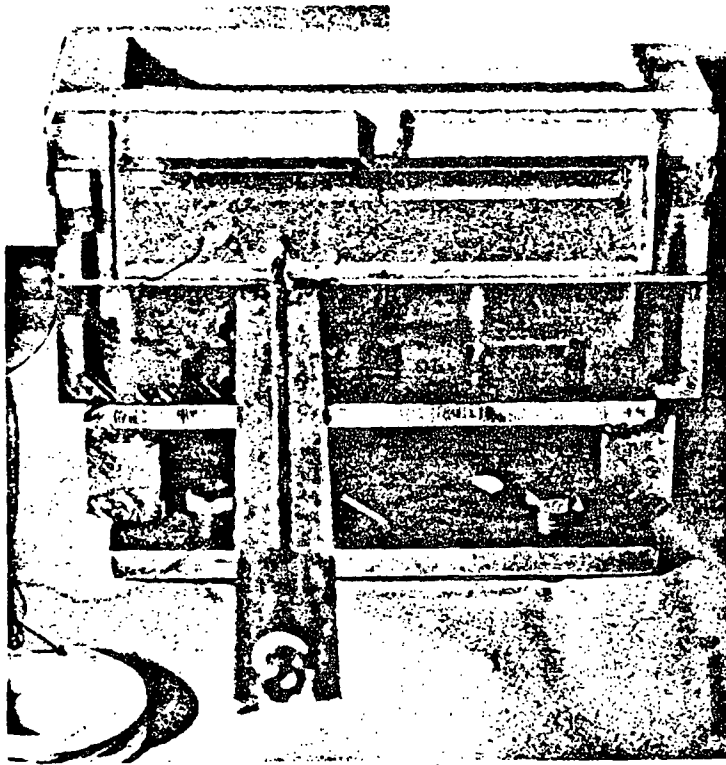


Figure 6. Picture of Rectangular Cavity with Probe and Thermistor.

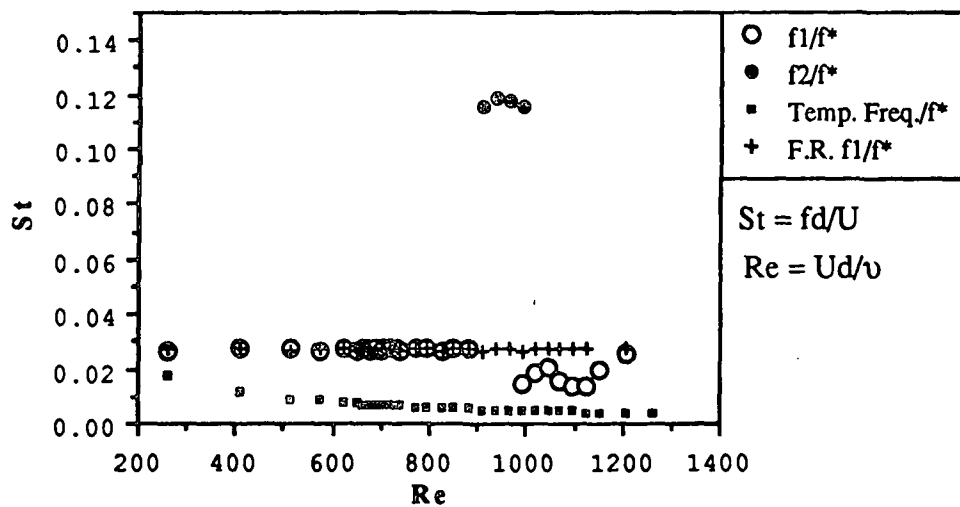


Figure 7. Strouhal vs. Reynolds Number.
 f_1 and f_2 at 100 Hz. Sampling Rate.

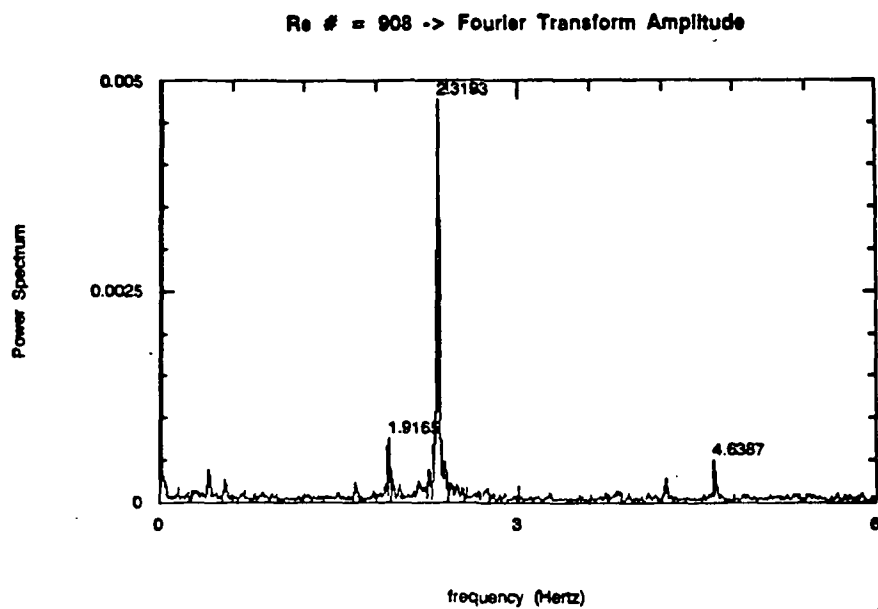


Figure 8. FFT Graph of Hot-Film Sensor Signal @ Re ~ 908.

(a)

Fourier Transform Amplitude (Re=804)

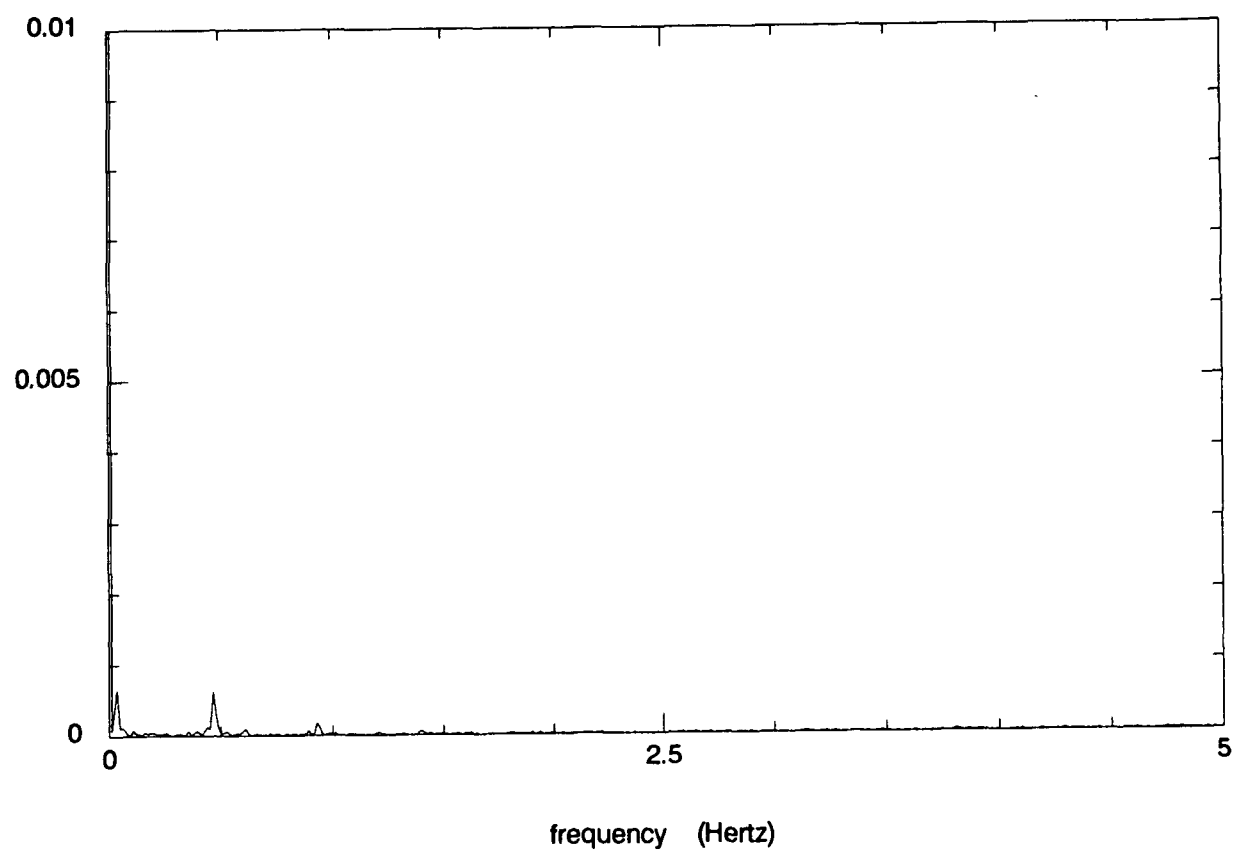


Figure 9a. Fourier transform amplitude of the hot-film anemometer signal at Re=804.

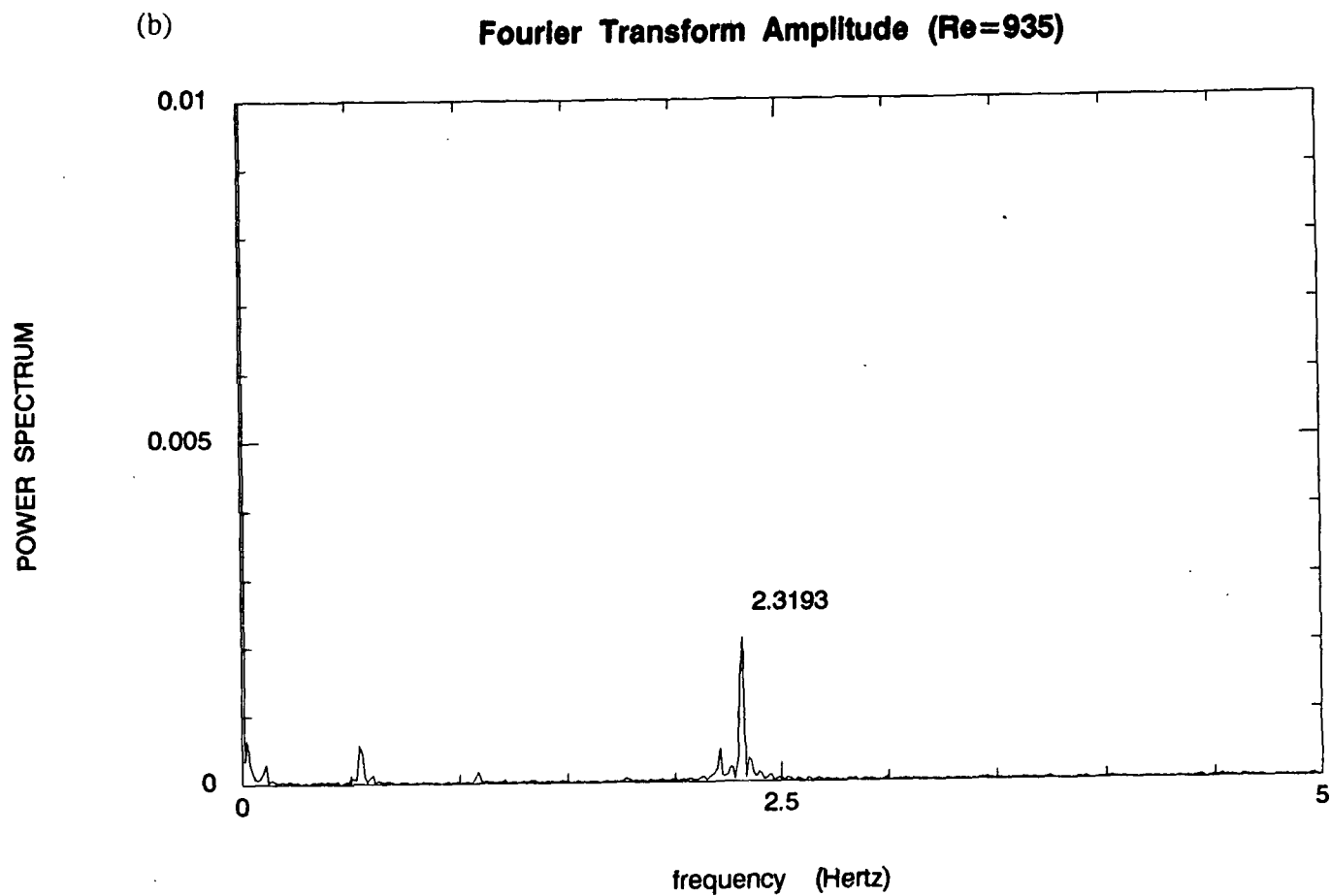


Figure 9b. Fourier transform amplitude of the hot-film anemometer signal at $Re=935$.

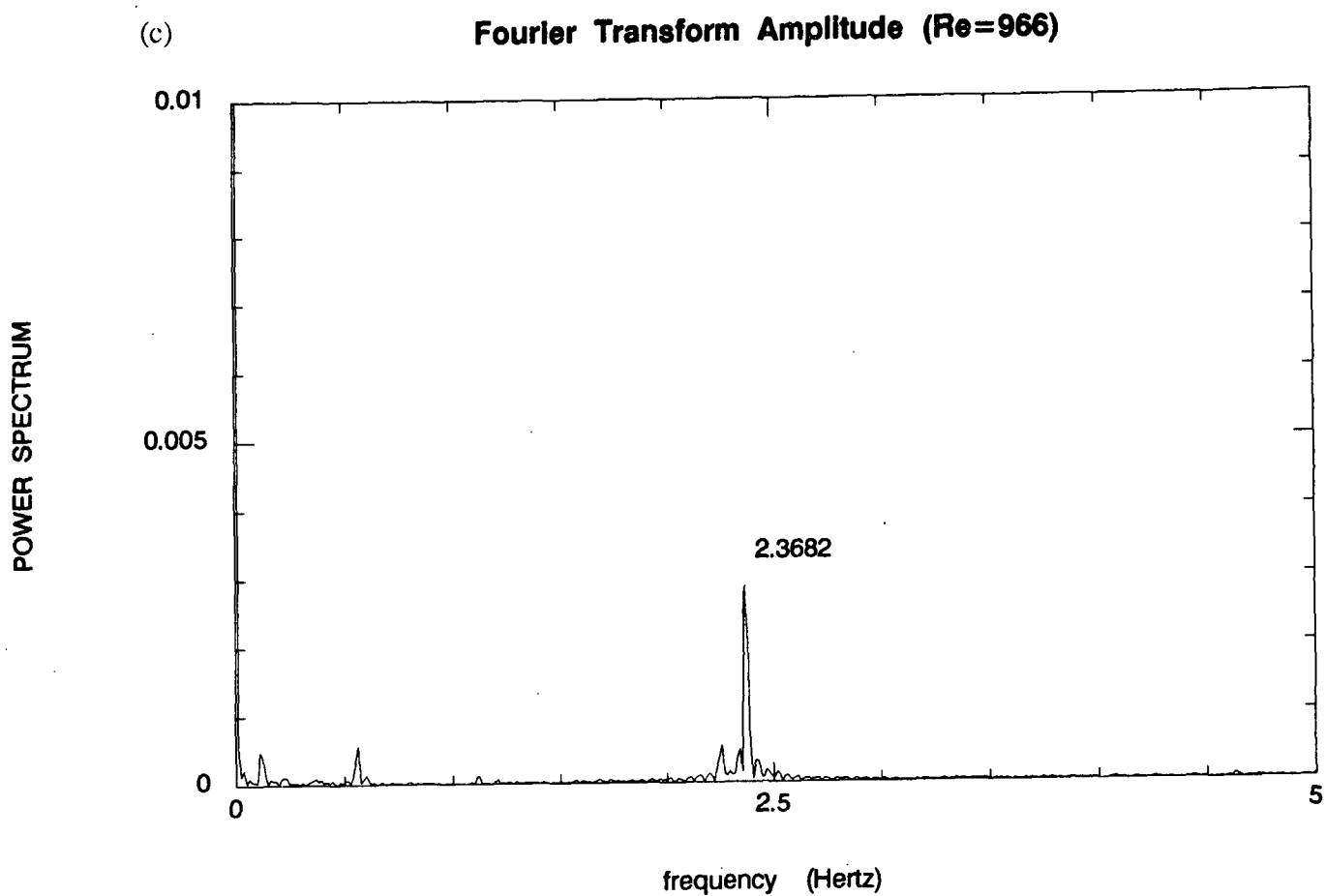


Figure 9c. Fourier transform amplitude of the hot-film anemometer signal at Re=966.

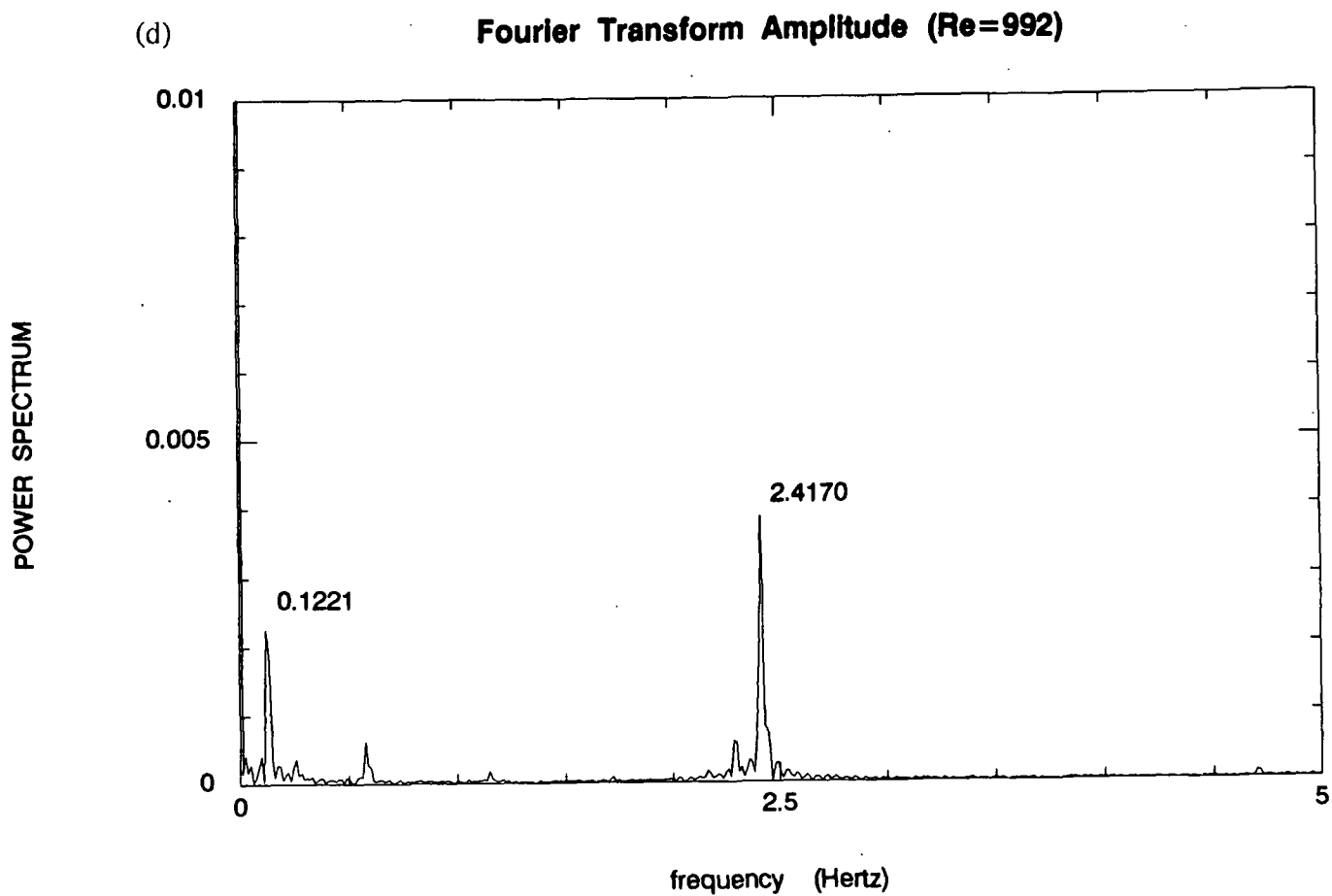


Figure 9d. Fourier transform amplitude of the hot-film anemometer signal at Re=992.

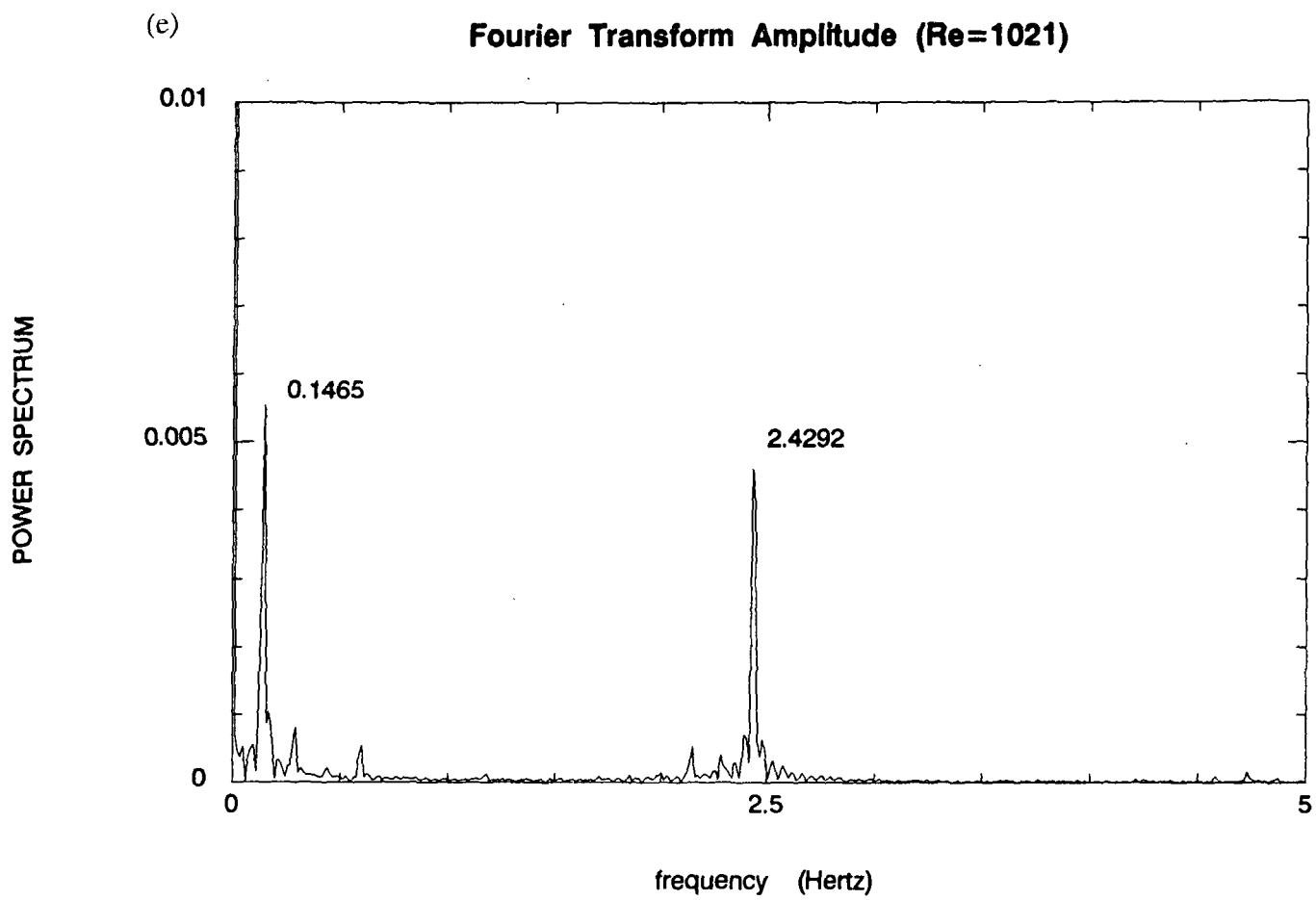


Figure 9e. Fourier transform amplitude of the hot-film anemometer signal at Re=1021.

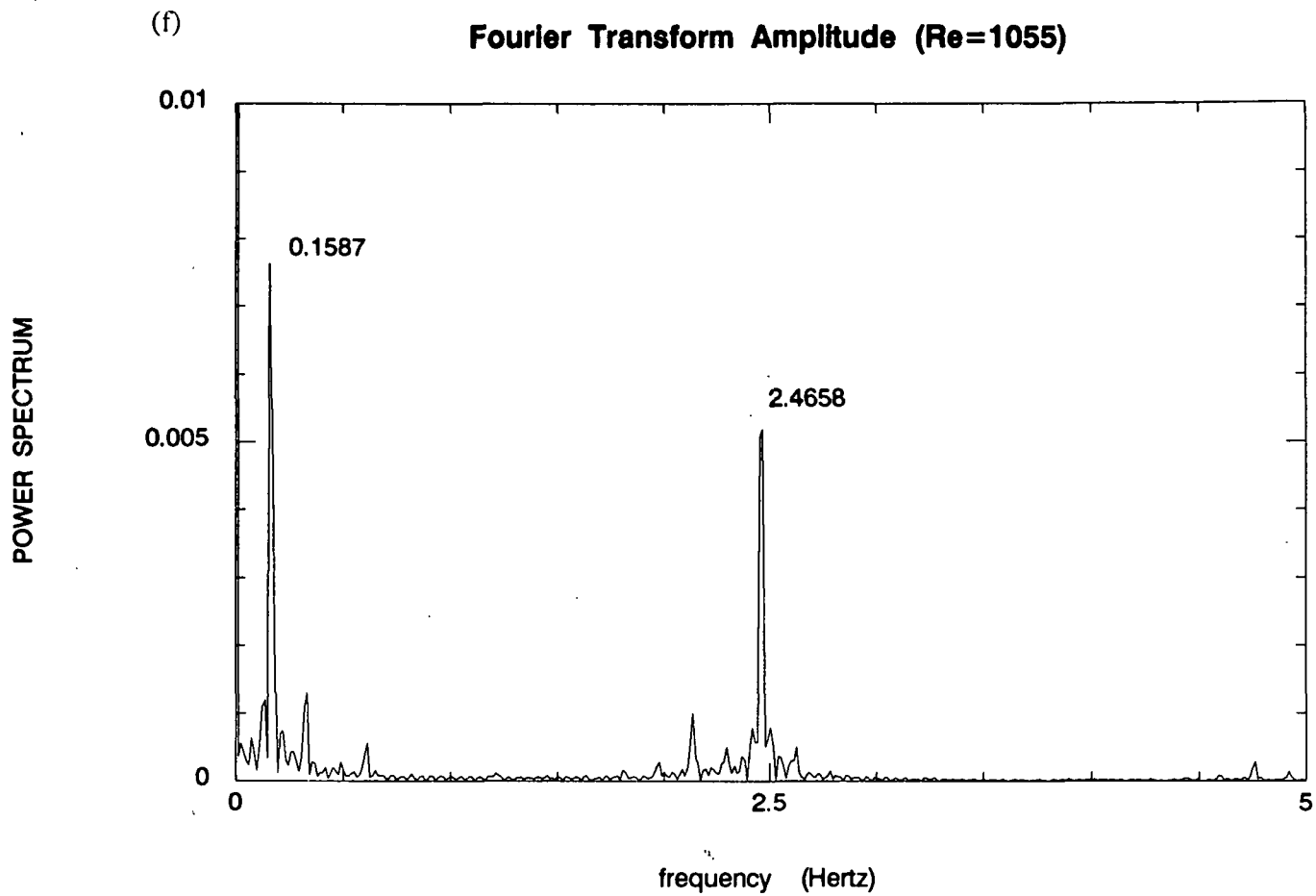


Figure 9f. Fourier transform amplitude of the hot-film anemometer signal at Re=1055.

(g)

Fourier Transform Amplitude (Re=1089)

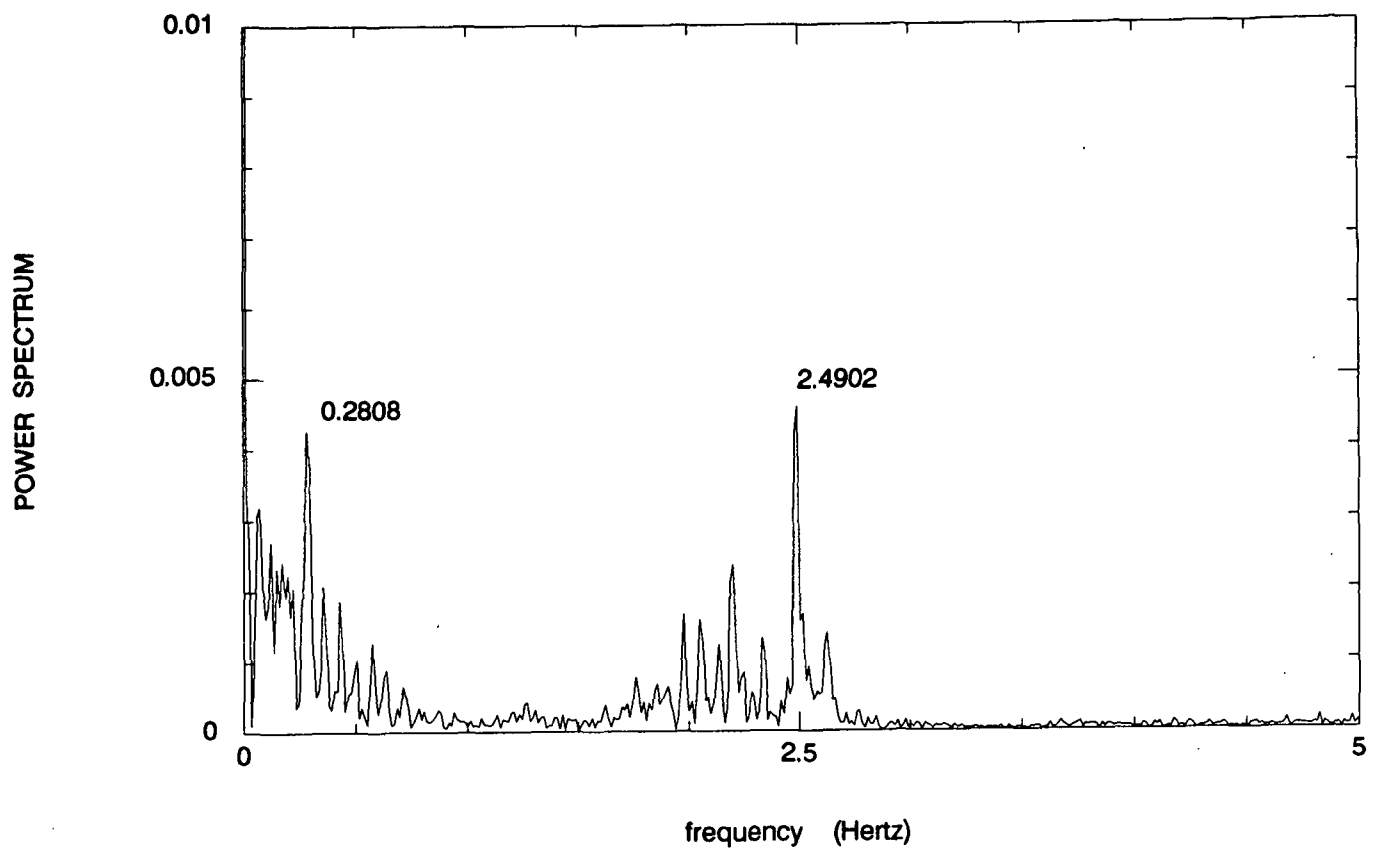


Figure 9g. Fourier transform amplitude of the hot-film anemometer signal at Re=1089.

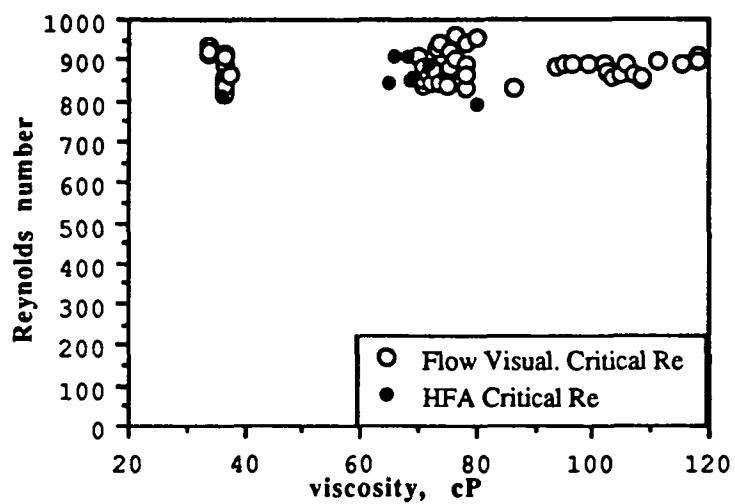


Figure 10. Comparisons of Critical Re
Between Flow Visualization and HFA Results.

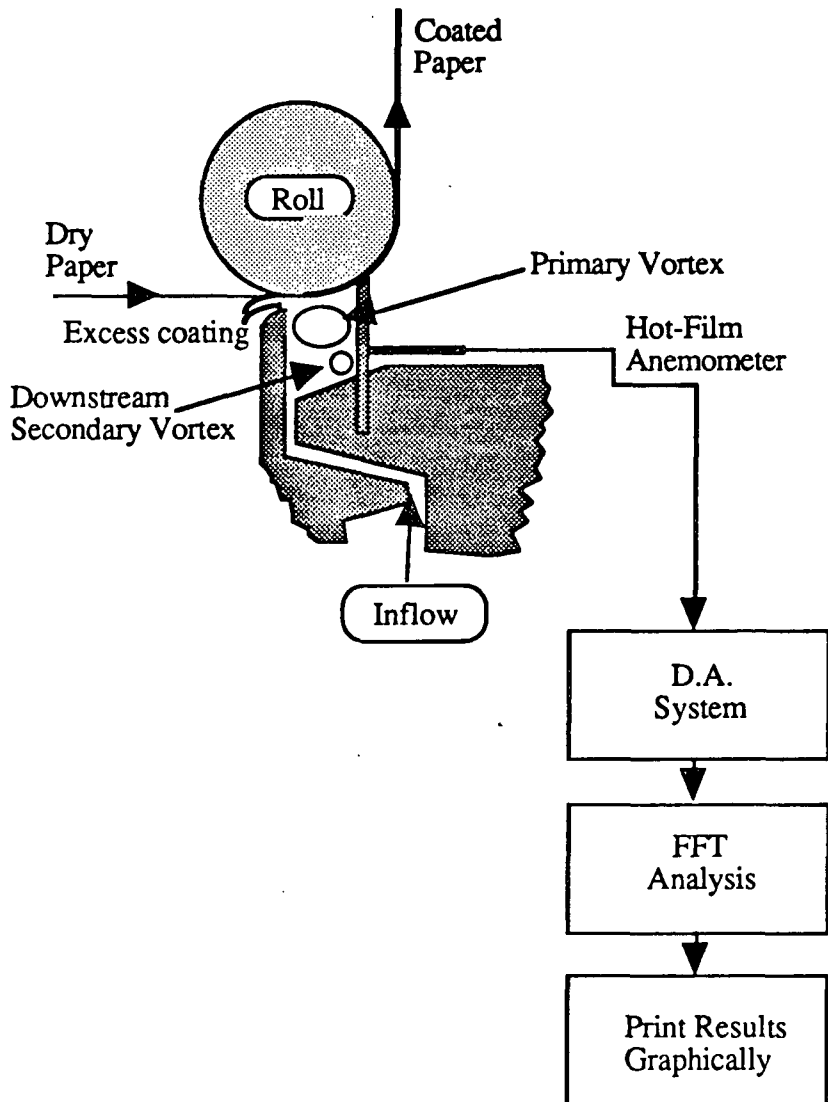


Figure 11. Example Schematic of Coater and HFA Setup.